Sensors and Actuators B 188 (2013) 354–359

Contents lists available at ScienceDirect

Sensors and Actuators B: Chemical

journal homepage: www.elsevier.com/locate/snb

Triazole functionalized gold nanoparticles for colorimetric Cr^{3+} sensing

Yu-Ching Chen, I-Lin Lee, Yi-Ming Sung, Shu-Pao Wu*

Department of Applied Chemistry, National Chiao Tung University, Hsinchu 300, Taiwan, ROC

ARTICLE INFO

Article history:
Received 24 April 2013
Received in revised form 21 June 2013
Accepted 25 June 2013
Available online 5 July 2013

Keywords:
Colorimetric sensor
Cr^{3+}
Gold nanoparticles
Triazole

ABSTRACT

Triazole functionalized gold nanoparticles (NTP@AuNPs) were synthesized through a click reaction and have been developed for sensitive and selective colorimetric Cr^{3+} detection. Gold nanoparticles were prepared by reducing $HAuCl_4$ with sodium citrate and then using 4-(*prop*-2-ynyloxy)*py*ridine (PP) as the capping agent. The acetylene part of PP and the azide part of 1-(azidomethyl)-4-nitrobenzene were combined to form a triazole structure through a click reaction. Aggregation of NTP@AuNPs was induced immediately in the presence of Cr^{3+} ions, yielding a color change from red to purple. This Cr^{3+}-induced aggregation of NTP@AuNPs was first monitored using the naked eye and then UV–vis spectroscopy with a detection limit of 1.4 μM. In addition, NTP@AuNPs were also used to detect Cr^{3+} in lake water samples, with low interference.

1. Introduction

Trivalent chromium, Cr^{3+}, is identified as an essential nutrient that regulates insulin action on the control of blood sugar, with a recommended daily intake 50–200 μg for adults [1–3]. The effect of chromium deficiency has been connected to insulin resistance or glucose intolerance. However, high levels of Cr^{3+} can induce oxidative damage to some cellular components, such as lipids, proteins, and DNA [4,5]. Due to its extensive applications, such as electroplating, alloying, and paint pigments, chromium ion is also an environmental pollutant. In order to detect chromium ions in biological and environmental samples, the design of highly selective and sensitive chromium sensors is an important issue.

There are several methods developed for detecting chromium ions in various samples, such as atomic absorption spectrometry (AA) [6,7], inductively coupled plasma-atomic emission spectrometry (ICP-AES) [8], inductively coupled plasma-mass spectrometry (ICP-MS) [9,10], and voltammetry [11]. These methods require expensive instruments and are not easily employed in the case of on-site assays. Recently, more attention is focused on the development of low-cost, selective, and sensitive methods for chromium detection, with several fluorescent chemosensors for Cr^{3+} detection reported [12–16]. Because they are made of organic molecules, they are not highly soluble in water and have higher detection limits. Herein, we report a simply prepared gold nanoparticle-based sensor for detecting Cr^{3+} over 15 other metal ions in an aqueous solution.

Gold nanoparticles (AuNPs) display typical surface plasmon resonance (SPR) absorption properties, which are extremely sensitive to size, shape, and interparticle distance [17,18]. Many AuNPs-based colorimetric sensors utilize the interparticle plasmon coupling upon the analyte-induced aggregation of AuNPs, which results in a color change from red to blue. In these assays, analyte-triggered aggregation of AuNPs leads to a red shift in the SPR absorption band, resulting in a red-to-blue color change. On the other hand, the removal of analyte results in the redispersion of the aggregated AuNPs, causing the color to revert from blue to red. The distance-dependent SPR absorption of AuNPs has become a useful tool for the development of colorimetric sensing of various analytes, such as metal ions [19–29], anions [30–32], proteins [33–35], and oligonucleotides [36,37].

In this report, triazole functionalized gold nanoparticles (NTP@AuNPs) were synthesized for detecting Cr^{3+}. The gold nanoparticles were prepared through the citrate-mediated reduction of $HAuCl_4$. 4-(Prop-2-ynyloxy)pyridine (PP) was attached to the surface of AuNPs through the pyridine nitrogen. Finally, the azide part of 1-(azidomethyl)-4-nitrobenzene and the acetylene part of PP were combined to form a triazole structure on the surface of AuNPs through a click reaction. The synthesized 4-{[1-(4-*n*itrobenzyl)-1H-1,2,3-*t*riazol-4-yl]oxy}*py*ridine@AuNPs (NTP@AuNPs) can be used for metal ion detection (Scheme 1). Metal ions such as Ag^+, Al^{3+}, Ca^{2+}, Cd^{2+}, Co^{2+}, Cu^{2+}, Cr^{3+}, Fe^{2+}, Fe^{3+}, Hg^{2+}, Mg^{2+}, Mn^{2+}, Ni^{2+}, Pb^{2+}, and Zn^{2+} were tested for metal ion selectivity but Cr^{3+} was the only metal ion that caused the aggregation of NTP@AuNPs. This caused the SPR

* Corresponding author. Tel.: +886 3 5712121x56506.
E-mail addresses: spwu@mail.nctu.edu.tw, spwu@faculty.nctu.edu.tw (S.-P. Wu).

0925-4005/$ – see front matter © 2013 Elsevier B.V. All rights reserved.
http://dx.doi.org/10.1016/j.snb.2013.06.088

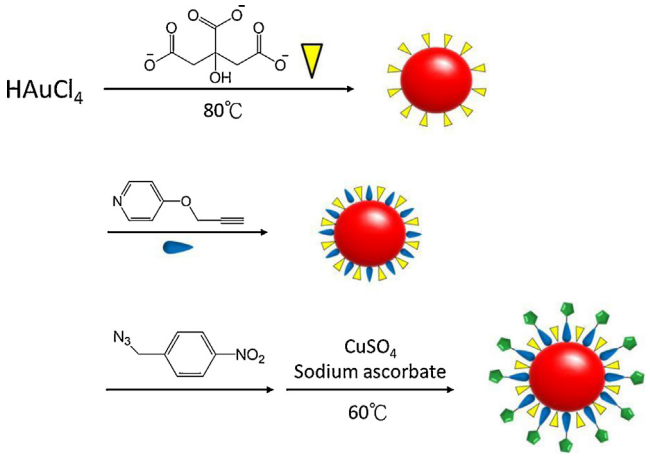

Scheme 1. Synthesis of NTP@AuNPs.

absorption band of NTP@AuNPs to shift to a longer wavelength, and consequently a color change from red to blue that can be used to detect the presence of Cr^{3+} ions. The SPR absorption at 639 nm directly indicated the degree of NTP@AuNP aggregation caused by the addition of Cr^{3+} ions.

2. Materials and methods

2.1. Materials

Hydrogen tetrachloroaurate(III) tetrahydrate and potassium carbonate were obtained from Showa. 4-Hydroxy pyridine, 3-bromopropyne, sodium ascorbate, $Al(ClO_4)_3{\cdot}9H_2O$, and $Cr(ClO_4)_3{\cdot}6H_2O$ were obtained from Alfa Aesar. Sodium citrate tribasic dihydrate, sodium azide, $CuSO_4{\cdot}5H_2O$, $Ca(ClO_4)_2{\cdot}4H_2O$, $Cd(ClO_4)_2{\cdot}xH_2O$, $CoCl_2{\cdot}6H_2O$, $Cu(BF_4)_2{\cdot}xH_2O$, $Fe(BF_4)_2{\cdot}6H_2O$, $FeCl_3{\cdot}6H_2O$, $Hg(ClO_4)_2{\cdot}xH_2O$, KBr, $Mg(ClO_4)_2{\cdot}6H_2O$, $Ni(O_2CCH_3)_2{\cdot}4H_2O$, and $Zn(BF_4)_2{\cdot}xH_2O$ were obtained from Sigma–Aldrich. $MnSO_4{\cdot}H_2O$ was obtained from Riedel-de Haen. The transition metal ions were dissolved in the deionized water and stored at room temperature. The synthesis and characterization of 4-(prop-2-ynyloxy) pyridine and 1-(azidomethyl)-4-nitrobenzene are described in the supporting information.

2.2. Instruments

UV–vis spectra were recorded on an Agilent 8453 UV-vis spectrometer. Infrared data were obtained on Bomem DA8.3 Fourier-Transform Infrared Spectrometer. TEM images were recorded from JEOL JEM-2010 Transmission Electro Microscope. ICP-MS data were recorded on an ICP-MS Perkin Elmer SCIEX ELAN 5000. NMR spectra were obtained on a Bruker DRX-300 NMR spectrometer.

2.3. Synthesis of NTP@AuNPs

Gold nanoparticles were prepared by reducing $HAuCl_4$ with trisodium citrate. All glassware was thoroughly cleaned with aqua regia (3:1 HCl/HNO_3) and rinsed with Millipore-Q water prior to use. Briefly, $HAuCl_4$ (80 mM, 200 μL) was added into 80 mL deioned water and heated it up to 80 °C. Trisodium citrate (38.8 mM, 2.784 mL) was then add in to the solution. The mixture was stirred for 30 min at the same temperature. 4-(Prop-2-ynyloxy)pyridine (PP) aqueous solution (0.01 M, 200 μL) was added into citrate modified AuNPs solution, stirring for 2 h at room temperature. PP@AuNPs were centrifuged for 20 min (14,200 rpm) and then suspended with Millipore-Q water. 1-(Azidomethyl)-4-nitrobenzene aqueous solution (0.01 M, 200 μL) was added into PP@AuNPs solution, stirring for 15 min. Copper sulfate (2 mM, 100 μL) and sodium ascorbic acid (20 mM, 100 μL) were added into PP@AuNPs solution and stirred for 3 h at 60 °C. The synthesized 4-{[1-(4-*n*itrobenzyl)-1H-1,2,3-*t*riazol-4-yl]oxy}*p*yridine@AuNPs (NTP@AuNPs) were dialysis with 3.5 K MWCO Spectra/Por 7 membranes. The finally dispersed NTP@AuNPs can be used for metal ions detection. The size of the NTP@AuNPs was verified by transmission electron microscope (TEM) analysis.

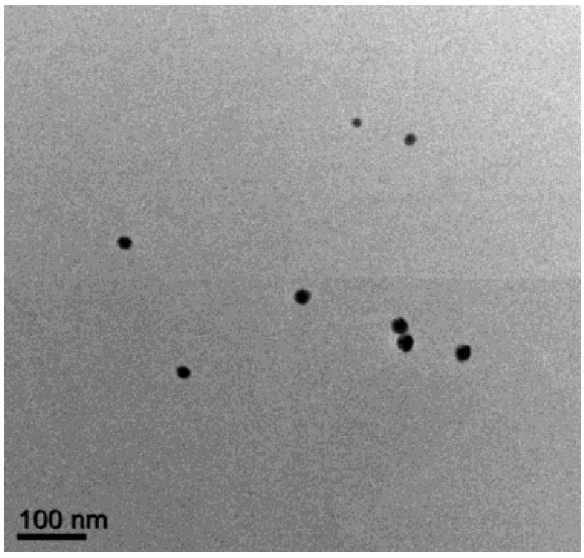

Fig. 1. TEM images of NTP@AuNPs. The scale bar is 100 nm.

2.4. Colorimetric detection of Cr^{3+} ions

To a 1.0 mL of solution containing NTP@AuNPs, different metal ions ($[M^{n+}] = 30$ μM) were added separately. The mixtures were maintained at room temperature for 10 min and then transferred separately into 1.5-mL quartz cuvette. Their SPR absorption bands were recorded by UV–vis spectrophotometer.

2.5. The influence of pH on Cr^{3+} induced aggregation of NTP@AuNPs

AuNPs were added with Cr^{3+} (30 μM) in 1.0 mL water solution (10 mM buffer). The buffers were: pH 3–4, $CH_3COOH/NaOH$; pH 4.5–7.0, MES/NaOH; pH 7.0–10, Hepes.

3. Results and discussion

3.1. Synthesis and characterization of NTP@AuNPs

Gold nanoparticles were prepared through the citrate-mediated reduction of $HAuCl_4$. 4-(Prop-2-ynyloxy)pyridine (PP) was added into the as-prepared AuNPs solution to be the capping agent. The azide part of 1-(azidomethyl)-4-nitrobenzene and the acetylene part of PP were combined to form a triazole structure under the click reaction. The synthesized NTP@AuNPs can be used for further studies (Scheme 1). Transmission electron microscopy (TEM) images revealed that the particle size of NTP@AuNPs is about 14 nm (Fig. 1). The cycloaddition products from the click reaction were verified by infrared spectroscopy. Fig. 2a shows characteristic absorption peaks of citrate@AuNPs at 1640 cm^{-1} (C=O) and 3000–3600 cm^{-1} (O—H). Fig. 2b clearly demonstrates that PP@AuNPs were obtained

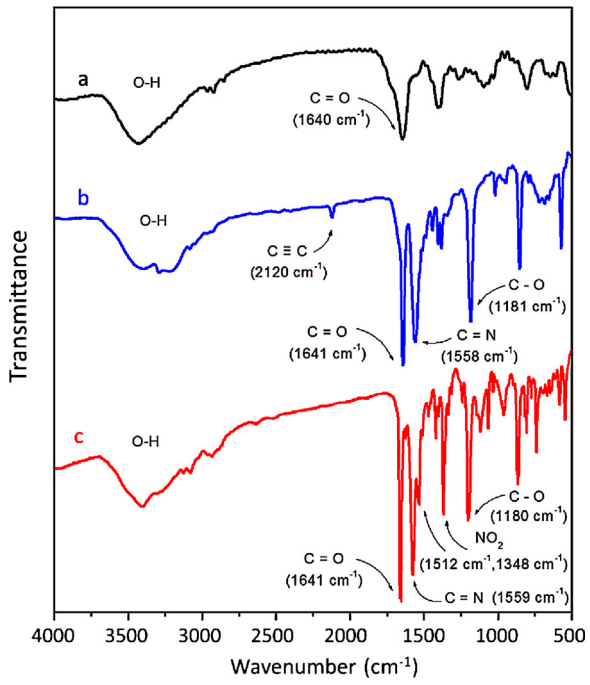

Fig. 2. FT-IR spectra of (a) citrate@AuNPs, (b) PP@AuNPs and (c) NTP@AuNPs.

due to peaks at 2120 cm^{-1} (—C≡CH) and 1181 cm^{-1} (C—O). In Fig. 2c, the peak that was originally at 2120 cm^{-1} (—C≡CH) has disappeared, and new peaks at 1512 cm^{-1} and 1348 cm^{-1} (NO_2) have appeared, indicating that the click reaction has proceeded on the surface of AuNPs.

3.2. Interaction of NTP@AuNPs with various metal Ions

The bonding performance of NTP@AuNPs with metal ions in aqueous solutions was tested. To evaluate the selectivity of NTP@AuNPs toward various metal ions, the absorption spectra of NTP@AuNPs were taken in the presence of several metal ions: Ag^{+}, Al^{3+}, Ca^{2+}, Cd^{2+}, Co^{2+}, Cu^{2+}, Fe^{2+}, Fe^{3+}, Hg^{2+}, Mg^{2+}, Mn^{2+}, Ni^{2+}, Pb^{2+}, and Zn^{2+}. Fig. 3 shows the effect of metal ions on the appearance of NTP@AuNPs in solution. Cr^{3+} was the only ion that resulted in an absorption peak shift, from 526 nm to 639 nm. This red shift could also be observed by the naked eye as a color change from red to blue. Other metal ions did not influence the absorption spectra, indicating that no aggregation occurred. The triazole groups on NTP@AuNPs function as metal ion binding ligands. Since Cr^{3+} was bound between the triazoles, the NTP@AuNPs aggregated (Scheme 2).

To gain a clearer understanding of the structure of NTP–Cr^{3+} complexes formed on the AuNPs, ^{1}H NMR spectroscopy was employed (Figure S1 in the supporting information). Cr^{3+} is a paramagnetic ion and can therefore affect the proton signals that are close to the Cr^{3+} binding site [38]. The ^{1}H NMR spectra of a NTP analog recorded with increasing amounts of Cr^{3+} show that the triazole proton (H_b) signal shifted downfield as more and more Cr^{3+} was added. This indicates that Cr^{3+} binds to NTP mainly through the nitrogen atom in a triazole.

Cr^{3+} triggered aggregation of NTP@AuNPs was mainly through two-step binding. The first step involves NTP binding to a Cr^{3+} ion through one nitrogen atom in a triazole. Secondly, bonds formed between Cr^{3+} and nitrogen atoms in another NTP capped onto adjacent AuNPs resulting in aggregation. Fig. 4 shows the TEM image of Cr^{3+} induced aggregation of NTP@AuNPs. Effectively, Cr^{3+} functioned as a bridge between particles, and triggered the aggregation of NTP@AuNPs.

The degree of aggregation of NTP@AuNPs depended on the concentration of Cr^{3+} ions; Fig. 5 shows the SPR absorption change with the addition of different concentrations of Cr^{3+}. The absorbance at 526 nm decreased with increasing Cr^{3+} concentration. A new band at 639 nm formed during Cr^{3+} titration as a result of the induced aggregation of AuNPs. A linear relationship was found when the concentration of Cr^{3+} ions was between 5 μM and 65 μM. The limit of detection for Cr^{3+} was found to be 1.4 μM (see Figure S2 in supplementary data).

Aggregated NTP@AuNPs can be redispersed by removing Cr^{3+} ions with EDTA; this was confirmed by the consequent SPR absorption shift from 639 nm to 526 nm (Fig. 6). After removing the

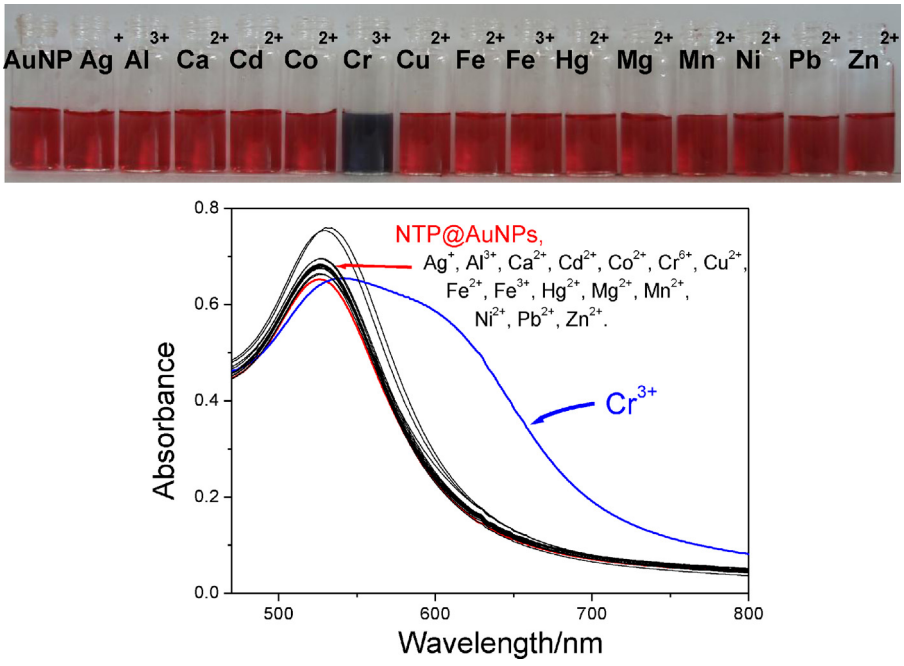

Fig. 3. (Top) Photographic images of NTP@AuNPs in the present of various metal ions. (Bottom) UV–vis spectra of NTP@AuNPs in the presence of different metal ions (30 μM).

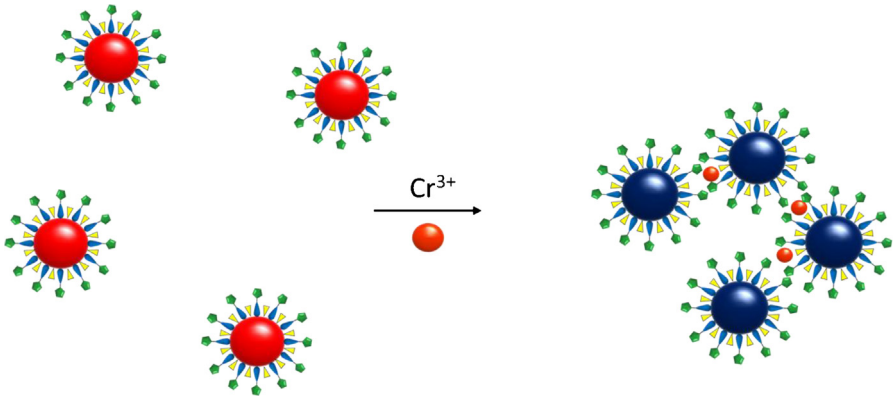

Scheme 2. Schematic depiction of the Cr^{3+}-triggered aggregation of NTP@AuNPs for Cr^{3+} detection.

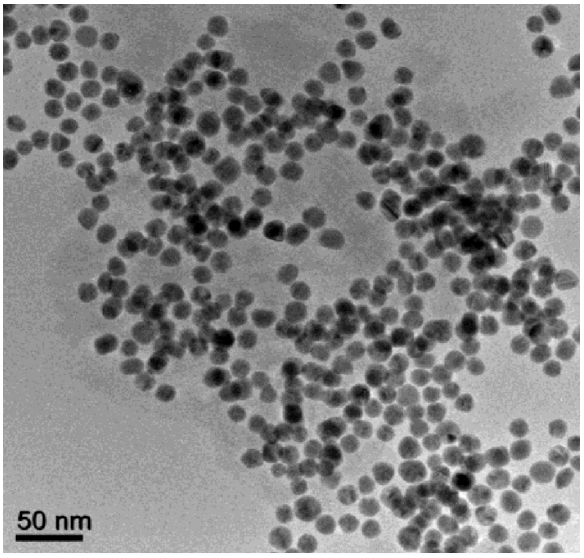

Fig. 4. TEM image of NTP@AuNPs in the presence of Cr^{3+} ions (30 μM).

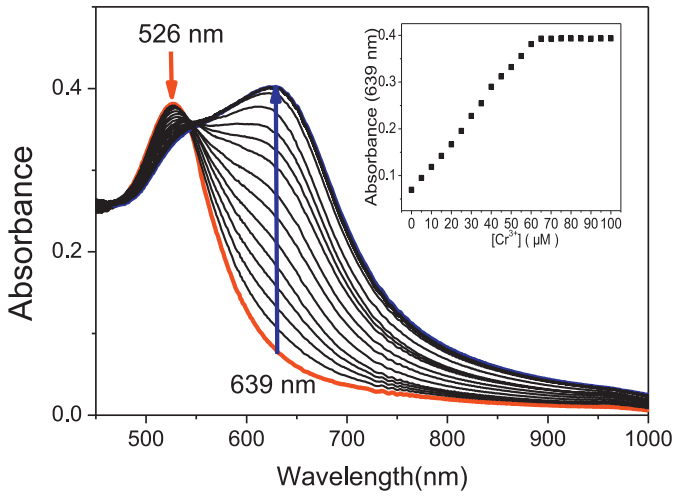

Fig. 5. Surface plasmon resonance absorption change of NTP@AuNPs in the presence of different concentrations of Cr^{3+}.

solution using a centrifuge and suspending it with an aqueous media, the dispersed NTP@AuNPs can be reused to detect Cr^{3+}. Through this technique, the NTP@AuNPs system can be used repeatedly for the detection of Cr^{3+}.

3.3. Interference studies

In order to study the influence of other metal ions on Cr^{3+} binding to NTP@AuNPs, competitive experiments were carried out in the presence of Cr^{3+} (30 μM) with other metal ions Ag^{+}, Al^{3+}, Ca^{2+}, Cd^{2+}, Co^{2+}, Cu^{2+}, Fe^{2+}, Fe^{3+}, Hg^{2+}, Mg^{2+}, Mn^{2+}, Ni^{2+}, Pb^{2+}, and Zn^{2+} at 30 μM each (Fig. 7). The SPR absorption shift caused by the mixture of Cr^{3+} with another metal ion was similar to that caused solely by Cr^{3+}. This indicates that other metal ions did not interfere in the binding of NTP@AuNPs with Cr^{3+}. This finding is consistent with previous studies suggesting that Cr^{3+} is the only metal ion that can induce the aggregation of NTP@AuNPs.

3.4. The influence of pH on Cr^{3+}-induced aggregation of NTP@AuNPs

To investigate the pH range in which NTP@AuNPs can effectively detect Cr^{3+}, a pH titration of NTP@AuNPs was carried out. In Fig. 8,

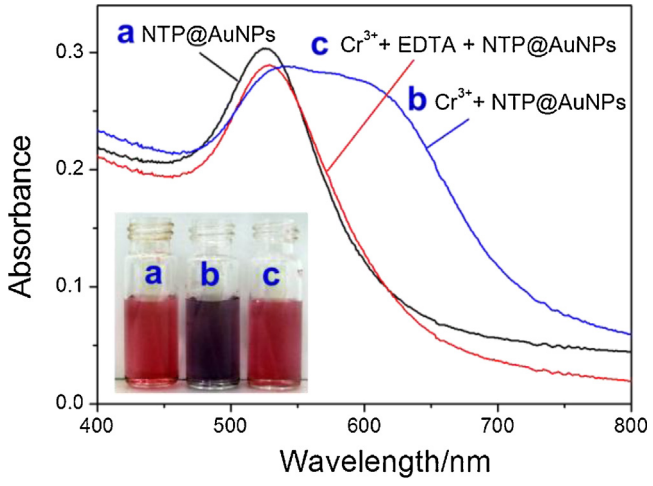

Fig. 6. Reversible binding of Cr^{3+} with NTP@AuNPs. (a) The black line is the UV–vis spectra of NTP@AuNPs. (b) The blue line is the UV–vis spectra of NTP@AuNPs in the presence of Cr^{3+} (30 μM). (c) The red line is the UV–vis spectra of NTP@AuNPs in the presence of Cr^{3+} (30 μM) followed by addition of EDTA (300 μM). (For interpretation of the references to color in this figure legend, the reader is referred to the web version of the article.)

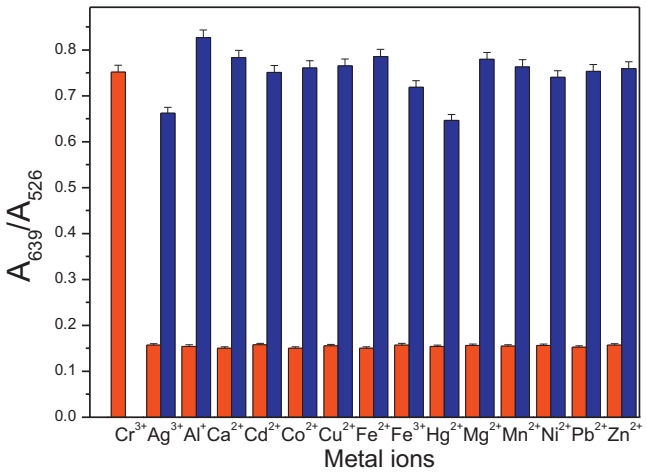

Fig. 7. Absorbance ratio ($A_{639\,nm}/A_{526\,nm}$) upon the addition of NTP@AuNPs to Cr^{3+} for the selected metal ions. Red bars represent the addition of single metal ion (30 μM); blue bars are the addition of Cr^{3+} (30 μM) with another metal ion (30 μM). (For interpretation of the references to color in this figure legend, the reader is referred to the web version of the article.)

the absorbance ratio (A_{639}/A_{526}) of NTP@AuNPs was low and constant in the pH range of 4–10. This indicates that NTP@AuNPs were stable in the pH range of 4–10. When the pH was lower than 4, the absorbance ratio (A_{639}/A_{526}) of NTP@AuNPs slightly increased. Under acidic conditions (pH = 3), protonation on NTP resulted in the aggregation of AuNPs. The influence of pH on Cr^{3+}-induced aggregation of NTP@AuNPs is shown in Fig. 8; addition of Cr^{3+} resulted in a high absorbance ratio (A_{639}/A_{526}) in a pH range of 4–7. At pH > 8, the absorbance ratio ($A_{639\,nm}/A_{526\,nm}$) decreased due to the formation of colloidal $Cr(OH)_3$. At pH 3, the absorbance ratio ($A_{639\,nm}/A_{526\,nm}$) was slightly higher than that at pH 4 because the acidic conditions (pH = 3) caused the aggregation of NTP@AuNPs. Therefore, the optimal pH range for detecting Cr^{3+} by NTP@AuNPs is in pH range of 4–7.

3.5. Application of NTP@AuNPs for the analysis of lake water samples

To confirm the practical application of NTP@AuNPs, water samples from different lakes located in Hsinchu, Taiwan were collected. All water samples were filtered through a 0.2 μm membrane and then spiked with different amounts of Cr^{3+} standard

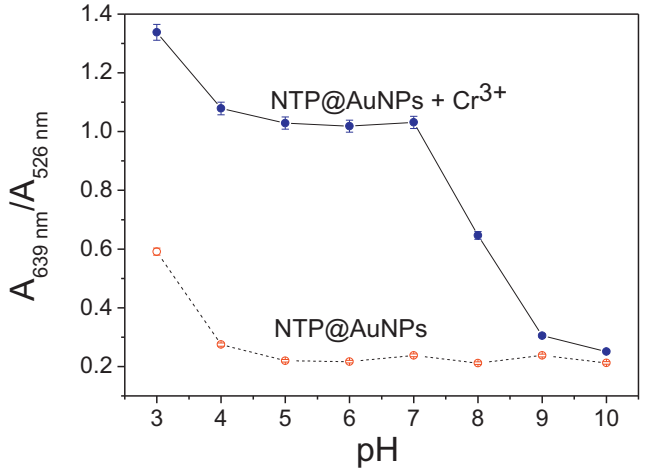

Fig. 8. Influence of pH on the UV/vis spectra of NTP@AuNPs in the absence and presence of Cr^{3+} (30 μM).

Table 1
Results of Cr^{3+} detection in lake water samples.

	ICP-MS	Proposed method[a]	Relative error (%)
Sample 1	$(28.24 \pm 0.05) \times 10^{-6}$ M	$(26.71 \pm 0.04) \times 10^{-6}$ M	5.42
Sample 2	$(39.46 \pm 0.05) \times 10^{-6}$ M	$(37.13 \pm 0.05) \times 10^{-6}$ M	5.90
Sample 3	$(51.25 \pm 0.09) \times 10^{-6}$ M	$(48.49 \pm 0.08) \times 10^{-6}$ M	5.39

[a] Using NTP@AuNPs.

solution. A calibration curve of NTP@AuNPs SPR shifts in the presence of different Cr^{3+} concentrations was prepared (see Figure S2 in supplementary data). The analytical results are shown in Table 1. The results obtained with NTP@AuNPs were in good agreement with those obtained using the inductively coupled plasma mass spectrometry (ICP-MS) method, with a relative error of less than 6%. These results indicate that the designed probe is applicable for Cr^{3+} detection in water samples.

4. Conclusion

In this report, we have used the color change caused by gold nanoparticles aggregation to develop a colorimetric method for Cr^{3+} detection. Cr^{3+} was the only metal ion that induced aggregation of NTP@AuNPs, which resulted in a color change from red to blue and a corresponding SPR absorption shift from 526 nm to 639 nm. This method provided a rapid and sensitive detection of Cr^{3+} in aqueous solution with a detection limit of 1.4 μM. The optimal pH range for Cr^{3+} detection using NTP@AuNPs was determined to be from 4 to 7. In addition, NTP@AuNPs were also applied to detect Cr^{3+} in lake water samples, with low interference.

Supplementary data

Synthesis of 4-(prop-2-ynyloxy)pyridine and 1-(azidomethyl)-4-nitrobenzene, and the calibration curve for the detection of Cr^{3+} by NTP@AuNPs.

Acknowledgements

We gratefully acknowledge the financial support of the National Science Council (ROC) and National Chiao Tung University.

Appendix A. Supplementary data

Supplementary data associated with this article can be found, in the online version, at http://dx.doi.org/10.1016/j.snb.2013.06.088.

References

[1] W.T. Cefalu, F.B. Hu, Role of chromium in human health and in diabetes, Diabetes Care 27 (2004) 2741–2751.
[2] R.A. Anderson, Chromium, glucose intolerance and diabetes, Journal of the American College of Nutrition 17 (1998) 548–555.
[3] W. Mertz, Chromium in human nutrition: a review, The Journal of Nutrition (1993) 626–633.
[4] O.Y. Vasylkiv, O.I. Kubrak, K.B. Storey, V.I. Lushchak, Cytotoxicity of chromium ions may be connected with induction of oxidative stress, Chemosphere 80 (2010) 1044–1049.
[5] O.V. Lushchak, O.I. Kubrak, O.V. Lozinsky, J.M. Storey, K.B. Storey, V.I. Lushchak, Chromium(III) induces oxidative stress in goldfish liver and kidney, Aquatic Toxicology 93 (2009) 45–52.
[6] Z. Wang, D. Fang, Q. Li, L. Zhang, R. Qian, Y. Zhu, H. Qu, Y. Du, Modified mesoporous silica materials for on-line separation and preconcentration of hexavalent chromium using a microcolumn coupled with flame atomic absorption spectrometry, Analytica Chimica Acta 725 (2012) 81–86.
[7] S. Sadeghi, A.Z. Moghaddam, Preconcentration and speciation of trace amounts of chromium in saline samples using temperature-controlled microextraction based on ionic liquid as extraction solvent and determination by electrothermal atomic absorption spectrometry, Talanta 99 (2012) 758–766.

[8] G. Cheng, M. He, H. Peng, B. Hu, Dithizone modified magnetic nanoparticles for fast and selective solid phase extraction of trace elements in environmental and biological samples prior to their determination by ICP-OES, Talanta 88 (2012) 507–515.
[9] Z. Chen, M. Megharaj, R. Naidu, Speciation of chromium in waste water using ion chromatography inductively coupled plasma mass spectrometry, Talanta 72 (2007) 394–400.
[10] H. Wang, X. Du, M. Wang, T. Wang, H. Ou-Yang, B. Wang, M. Zhu, Y. Wang, G. Jia, W. Feng, Using ion-pair reversed-phase HPLC ICP-MS to simultaneously determine Cr(III) and Cr(VI) in urine of chromate workers, Talanta 81 (2010) 1856–1860.
[11] R.T. Kachoosangi, R.G. Compton, Voltammetric determination of chromium(VI) using a gold film modified carbon composite electrode, Sensors and Actuators B: Chemical 178 (2013) 555–562.
[12] K. Huang, H. Yang, Z. Zhou, M. Yu, F. Li, X. Gao, T. Yi, C. Huang, Multisignal chemosensor for Cr^{3+} and its application in bioimaging, Organic Letters 10 (2008) 2557–2560.
[13] Z. Zhou, M. Yu, H. Yang, K. Huang, F. Li, T. Yi, C. Huang, FRET-based sensor for imaging chromium(III) in living cells, Chemical Communication (2008) 3387–3389.
[14] A.J. Weerasinghe, C. Schmiesing, E. Sinn, Highly sensitive and selective reversible sensor for the detection of Cr^{3+}, Tetrahedron Letters 50 (2009) 6407–6410.
[15] Z. Li, W. Zhao, Y. Zhang, L. Zhang, M. Yu, J. Liu, H. Zhang, An 'offeon' fluorescent chemosensor of selectivity to Cr^{3+} and its application to MCF-7 cells, Tetrahedron 67 (2011) 7096–7100.
[16] P. Saluja, N. Kaur, N. Singh, D.O. Jang, Benzimidazole-based fluorescent sensors for Cr^{3+} and their resultant complexes for sensing HSO_4^- and F^-, Tetrahedron 68 (2012) 8551–8556.
[17] C. Burda, X. Chen, R. Narayanan, M.A. El-Sayed, Chemistry and properties of nanocrystals of different Shapes, Chemical Review 105 (2005) 1025–1102.
[18] M.-C. Daniel, D. Astruc, Gold nanoparticles: assembly, supramolecular chemistry, quantum-size-related properties, and applications toward biology, catalysis, and nanotechnology, Chemical Review 104 (2004) 293–346.
[19] C.J. Murphy, A.M. Gole, S.E. Hunyadi, J.W. Stone, P.N. Sisco, A. Alkilany, B.E. Kinard, P. Hankins, Chemical sensing and imaging with metallic nanorods, Chemical Communication (2008) 544–557.
[20] Z. Jiang, Y. Fan, M. Chen, A. Liang, X. Liao, G. Wen, X. Shen, X. He, H. Pan, H. Jiang, Resonance scattering spectral detection of trace Hg^{2+} using aptamer-modified nanogold as probe and nanocatalyst, Analytical Chemistry 81 (2009) 5439–5445.
[21] Y.Q. Dang, H.W. Li, B. Wang, L. Li, Y.Q. Wu, Selective detection of trace Cr^{3+} in aqueous solution by using 5,5′-dithiobis (2-nitrobenzoic acid)-modified gold nanoparticles, ACS Applied Materials & Interfaces 1 (2009) 1533–1538.
[22] Y. Yao, D. Tian, H. Li, Cooperative binding of bifunctionalized and click-synthesized silver nanoparticles for volorimetric Co^{2+} sensing, ACS Applied Materials & Interfaces 2 (2010) 684–690.
[23] X. Li, J. Wang, L. Sun, Z. Wang, Gold nanoparticle-based colorimetric assay for selective detection of aluminium cation on living cellular surfaces, Chemical Communication 46 (2010) 988–990.
[24] S. Wu, Y. Chen, Y. Sung, Colorimetric detection of Fe^{3+} ions using pyrophosphate functionalized gold nanoparticles, Analyst 136 (2011) 1887–1891.
[25] S. Chen, Y.M. Fang, Q. Xiao, J. Li, S.B. Li, H.J. Chen, J.J. Sun, H.H. Yang, Rapid visual detection of aluminium ion using citrate capped gold nanoparticles, Analyst 137 (2012) 2021–2023.
[26] L. Zhao, Y. Jin, Z. Yan, Y. Liu, H. Zhu, Novel, highly selective detection of Cr(III) in aqueous solution based on a gold nanoparticles colorimetric assay and its application for determining Cr(VI), Analytica Chimica Acta 731 (2012) 75–81.
[27] S.K. Tripathy, J.Y. Woo, C.-S. Han, Colorimetric detection of Fe(III) ions using label-free gold nanoparticles and acidic thiourea mixture, Sensors and Actuators B: Chemical 181 (2013) 114–118.
[28] R. Liu, Z. Chen, S. Wang, C. Qu, L. Chen, Z. Wang, Colorimetric sensing of copper(II) based on catalytic etching of gold nanoparticles, Talanta 112 (2013) 37–42.
[29] L. Chen, X. Fu, W. Lu, L. Chen, Highly sensitive and selective colorimetric sensing of Hg^{2+} based on the morphology transition of silver nanoprisms, ACS Applied Materials & Interfaces 5 (2013) 284–290.
[30] K. Youk, K.M. Kim, A. Chatterjee, K.H. Ahn, Selective recognition of fumarate from maleate with a gold nanoparticle-based colorimetric sensing system, Tetrahedron Letters 49 (2008) 3652–3655.
[31] W.L. Daniel, M.S. Han, J.S. Lee, C.A. Mirkin, Colorimetric nitrite and nitrate detection with gold nanoparticle probes and kinetic end points, Journal of American Chemical Society 131 (2009) 6362–6363.
[32] L. Chen, W. Lu, X. Wang, L. Chen, A highly selective and sensitive colorimetric sensor for iodide detection based on anti-aggregation of gold nanoparticles, Sensors and Actuators B: Chemical 182 (2013) 482–488.
[33] C.S. Tsai, T.B. Yu, C.T. Chen, Gold nanoparticle-based competitive colorimetric assay for detection of protein–protein interactions, Chemical Communication (2005) 4273–4275.
[34] X. Xu, M.S. Han, C.A. Mirkin, A gold-nanoparticle-based real-time colorimetric screening method for endonuclease activity and inhibition, Angewandte Chemie, International Edition 46 (2007) 3468–3470.
[35] A. Laromiane, L. Koh, M. Murugesan, R.V. Ulijin, M.M. Stevens, Protease-triggered dispersion of nanoparticle assemblies, Journal of American Chemical Society 129 (2007) 4156–4157.
[36] C.A. Mirkin, R.L. Letsinger, R.C. Mucic, J.J. Storhoff, A DNA-based method for rationally assembling nanoparticles into macroscopic materials, Nature 382 (1996) 607–609.
[37] H.X. Li, L. Rothberg, Colorimetric detection of DNA sequences based on electrostatic interactions with unmodified gold nanoparticles, Proceedings of the National Academy of Sciences of the United States of America 101 (2004) 14036–14039.
[38] A. Harton, K. Terrell, J.C. Huffman, C. MacDonald, A. Beatty, S. Li, C.J. O'Connor, J.B. Vincent, Synthesis and characterization of novel oxo-bridged dinuclear and hydroxo-bridged trinuclear Chromium(III) assemblies, Inorganic Chemistry 36 (1997) 4875–4882.

Biographies

Yu-Ching Chen had MS in 2012, Department of Applied Chemistry at National Chiao Tung University.

I.-Lin Lee is studying for MS in the Department of Applied Chemistry at National Chiao Tung University.

Yi-Ming Sung is studying for PhD in the Department of Applied Chemistry at National Chiao Tung University.

Dr. Shu-Pao Wu had PhD in 2004, Department of Chemistry, The Ohio State University, USA; Adviser: J.A. Cowan, Postdoctoral Fellow, 2004–2006, College of Chemistry, University of California, Berkeley, USA; Adviser: J.P. Klinman, Assistant Professor, 2006, National Chiao Tung University, Taiwan, Republic of China. Current interests: metal ion chemosensors and AlkB.